

## Horizontal Eddy Fluxes of Momentum and Kinetic Energy in the Near-Surface of the Kuroshio Extension

HIDEO NISHIDA

*Hydrographic Department of Japan, Tsukiji, Chuo-Ku, Tokyo, Japan 104*

WARREN B. WHITE

*Scripps Institution of Oceanography, University of California, San Diego, La Jolla 92093*

(Manuscript received 23 June 1980, in final form 20 August 1981)

### ABSTRACT

Sequential monthly-mean temperature fields in the mid-latitude western North Pacific (30–45°N, 140–180°E), constructed from TRANSPAC XBT (expendable bathythermograph) data over a two-year period, are employed to analyze the interaction between mesoscale variability and the mean flow of the Kuroshio Extension. An empirical temperature–dynamic height regression, and the geostrophic approximation, lead to the computation of mean and eddy horizontal velocity components over the region, from which horizontal eddy processes in both the mean momentum and the mean kinetic energy balances of the Kuroshio Extension are estimated.

The Kuroshio Extension generally loses mean kinetic energy as it travels from the coast of Japan from 140 to 180°E, with much larger eddy kinetic energy west of the Shatsky Rise (160°E) than east of there. Concentrating upon zonally-averaged quantities in both subregions east and west of the Shatsky Rise, horizontal eddy momentum fluxes due to transient mesoscale variability (i.e.,  $\langle \bar{u}'v' \rangle$ ) tend to converge the mean eastward momentum. However, in the western subregion, quasi-stationary meanders in the mean flow are associated with a horizontal eddy momentum flux (i.e.,  $\langle \bar{u}'v' \rangle$ ) that reduces this tendency. The horizontal kinetic energy exchange between mean flow and mesoscale variability (e.g.,  $\langle \bar{u}'v'\partial\bar{u}/\partial y \rangle$ ) tends to increase the mean kinetic energy on the north side of the axis of mean flow and to decrease it on the south side, both east and west of the Shatsky Rise. On the other hand, the horizontal mean kinetic energy redistribution by horizontal eddy processes (e.g.,  $\langle -\partial/\partial y(\bar{u}'v'\bar{u}) \rangle$ ) tends to increase mean kinetic energy overall in the subregion east of the Shatsky Rise, showing little effect west of there. The net tendency upon the mean kinetic energy balance by these two horizontal eddy processes (i.e. exchange and redistribution) is to increase mean kinetic energy in the region east of the Shatsky Rise, with no significant effect west of there. Therefore, the reduction in mean kinetic energy from west to east along the Kuroshio Extension is not due to horizontal eddy processes.

### 1. Introduction

The role of eddy processes in the dynamics of the oceanic general circulation has, over the last decade, become an important subject of study. Several field investigations have been conducted, yielding time sequences of observations, taken over selected regions of the ocean, from which horizontal eddy processes in the mean kinetic energy balance have been computed. Webster (1961, 1965), using GEK data in the Gulf Stream south of Cape Hatteras, determined that horizontal cross-stream terms (i.e.,  $\bar{u}'v'$ ,  $\partial\bar{v}/\partial x$ ) in the mean kinetic energy balance of the Gulf Stream had a tendency to intensify the mean flow. Other works, using GEK data in the Kuroshio south of Japan (Szabo and Weatherly, 1979) and ship-drift data in the Gulf Stream (Hager, 1977), determined that horizontal downstream terms (e.g.  $\bar{u}'^2\partial\bar{u}/\partial x$ ) in the mean kinetic energy balance were important, tending both to intensify and to de-intensify the mean

flow. An array of submerged current meters has proved useful in revealing information on horizontal eddy processes (Schmitz, 1977) in the Gulf Stream south of the Grand Banks, where horizontal cross-stream terms in the mean kinetic energy balance tended to intensify the mean flow in deep water.

The present study seeks basic understanding on the interaction of mesoscale variability and the mean flow of the Kuroshio Extension east of Japan. This is made possible by computation of horizontal geostrophic velocities in the area from knowledge of the vertical and horizontal temperature structure of mesoscale variability. The TRANSPAC volunteer-observing-ship XBT program provides an adequate data base for making these calculations. It extends over the region 140–180°E, 30–45°N and allows mesoscale variability to be resolved each month for two years, on a spatial grid of 100 km (White and Bernstein, 1979). This degree of resolution leads to the estimation of horizontal eddy processes that af-

fect both the mean momentum and mean kinetic energy balances of the Kuroshio Extension.

Basic formulation of the mean kinetic energy balance can be developed as follows (e.g., Lumley and Panofsky, 1964): The momentum equation of mean flow in tensor notation, using the Boussinesq approximation, is given by

$$\begin{aligned} \frac{\partial \bar{u}_i}{\partial t} + \bar{u}_j \frac{\partial \bar{u}_i}{\partial x_j} = & -2\epsilon_{ijk} \Omega_j \bar{u}_k - \frac{1}{\rho_0} \frac{\partial \bar{p}}{\partial x_j} \delta_{ij} \\ & - \frac{\partial}{\partial x_j} \overline{u'_i u'_j} + A_H \frac{\partial^2 \bar{u}_i}{\partial x_\lambda \partial x_\lambda} \\ & + A_v \frac{\partial^2 \bar{u}_i}{\partial z^2} - \frac{\bar{\rho}}{\rho_0} g \delta_{i3}, \end{aligned} \quad (i, j, k = 1, 2, 3; \lambda = 1, 2) \quad (1.1)$$

where  $p$  and  $\rho$  denote departures from their static values (i.e.,  $p_0$  and  $\rho_0$ ), the bar denotes time mean, and the prime the departure from this mean.  $A$  is an eddy viscosity coefficient representing interaction with subgrid variability. The third term in this expression represents the effect of mesoscale variability upon mean flow.

The mean kinetic energy equation in tensor notation is obtained by multiplying (1.1) by  $\bar{u}_i$  (Harrison and Robinson, 1978), i.e.,

$$\begin{aligned} \frac{\partial}{\partial t} \left( \frac{\bar{u}_i \cdot \bar{u}_i}{2} \right) + \bar{u}_j \frac{\partial}{\partial x_j} \left( \frac{\bar{u}_i \cdot \bar{u}_i}{2} \right) = & - \frac{1}{\rho_0} \frac{\partial \bar{p}}{\partial x_j} \bar{u}_i \delta_{ij} \\ & - \bar{u}_i \frac{\partial}{\partial x_j} \overline{u'_i u'_j} + A_H \bar{u}_i \frac{\partial^2 \bar{u}_i}{\partial x_\lambda \partial x_\lambda} + A_v \bar{u}_i \frac{\partial^2 \bar{u}_i}{\partial z^2} \\ & - g \frac{\bar{\rho}}{\rho_0} \bar{u}_i \delta_{i3}. \end{aligned} \quad (1.2)$$

The second term in the right-hand side of (1.2) contains the effect of eddy processes; it can be separated into two parts, i.e.,

$$-\bar{u}_i \frac{\partial}{\partial x_j} \overline{u'_i u'_j} = - \frac{\partial}{\partial x} (\overline{u'_i u'_j} \cdot \bar{u}_i) + \overline{u'_i u'_j} \frac{\partial \bar{u}_i}{\partial x_j}. \quad (1.3)$$

The first term on the right-hand side of (1.3) represents divergence of transport of mean kinetic energy by eddy processes. This term integrates to zero over a domain, if on the boundary of the domain no flux of mean kinetic energy exists (i.e.,  $\overline{u'_i u'_j} \cdot \bar{u}_i = 0$ ). Therefore, this term acts only to redistribute mean kinetic energy inside the domain. The second term in (1.3) represents the rate of kinetic energy exchange between mean flow and mesoscale variability within the domain, yielding a source or sink of mean kinetic energy.

This study concentrates upon the role that *horizontal* eddy processes play in transporting momentum and in redistributing and exchanging mean ki-

netic energy. In Section 3, the streamline patterns of mean flow, as well as those of mean and eddy kinetic energy are displayed, yielding the basic horizontal statistical structure of the Kuroshio Extension. Since consideration of statistical significance does not allow an analysis of momentum and kinetic energy tendencies at each grid point, discussion is concentrated upon the zonally-averaged quantities of horizontal eddy processes. The zonal average is divided into two parts, upstream and downstream of the Shatsky Rise (160°E), chosen on the basis of the visibly apparent differences in the basic horizontal statistical structure of these two subregions. Section 4 deals with the horizontal momentum flux by transient mesoscale variability (Reynolds stresses), and Section 5 deals with that due to quasi-stationary meanders. In Section 6, terms in the mean kinetic energy balance are displayed, with both exchange and redistribution of mean kinetic energy by horizontal eddy processes computed, as well as the horizontal mean kinetic energy advection.

## 2. Data

Temperature data used in this study have been collected by the TRANSPAC XBT field program. These data have been mapped to yield a temperature field at 300 m for each month over the area of interest. Temperature values were interpolated to each half-degree grid point over this region using the method explained in Bernstein and White (1981). Dynamic height anomaly (100/1000 db) at each grid point was estimated using an empirical regression curve with 300 m temperature, constructed from the historical NODC hydrographic file (Bernstein and White, 1981). Estimated dynamic height anomalies are used to calculate near-surface current velocities using the geostrophic relation. Near-surface current velocities estimated in the above procedure serve as a basis for the subsequent analysis of horizontal eddy processes.

Twenty-four months (December 1976–November 1978) have been chosen for the present analysis, which ideally produces 24 velocity samples at each grid point in the field. But, not all months have full data coverage over the region of interest (30–45°N, 140–180°E). For example, in the northwestern part of the area, XBT data were sparse, giving very few samples. In the main part of the Kuroshio Extension (30–40°N), the data coverage was not sparse, and generally over 20 samples at each grid point have been obtained. Grid points with <10 samples have been excluded from the analysis.

Errors in this analysis are estimated as follows. As a first step, temperature errors in the mapped 300 m temperature field for each month were estimated by White and Bernstein (1979) to be  $\pm 0.7^\circ\text{C}$ . According to regression curves in Bernstein and White

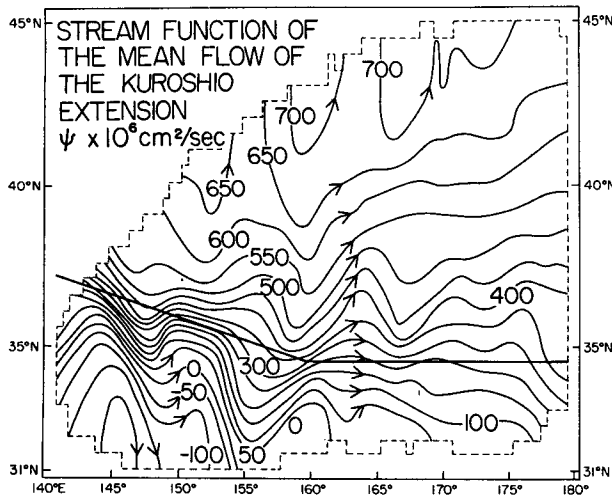


FIG. 1. Horizontal distribution of the mean flow as inferred from horizontal streamlines. Contour interval of the stream function exceeds twice the standard error.

(1981), relating 300 m temperature to dynamic height anomaly (100/1000 db),  $\pm 0.7^\circ\text{C}$  corresponds to  $\pm 4.5$  dynamic cm near  $10^\circ\text{C}$ . The regression curve itself has a standard deviation of 4.4 dynamic cm; therefore, the error ( $\sigma_0$ ) due to both of these sources is estimated to be  $\sigma_0 = 6.3$  dynamic cm. The propagation of the dynamic height anomaly error into geostrophic velocity yields an error in the latter ( $\sigma_u, \sigma_v$ ) of  $\pm 8.9 \text{ cm s}^{-1}$ . Further propagation of errors in the various terms important to the horizontal mean kinetic energy balance yields the following error estimates as examples:

$$\left. \begin{aligned} \sigma_{\overline{u'v'}}^2 &= \frac{1}{N} \sum_{i=1}^N [(u')^2 \sigma_{v'}^2 + (v')^2 \sigma_{u'}^2] \\ \sigma_{\overline{u'v'}(\partial \overline{u}/\partial y)} &= (\overline{u'v'})^2 \sigma_{\partial \overline{u}/\partial y}^2 + \left(\frac{\partial \overline{u}}{\partial y}\right)^2 \sigma_{\overline{u'v'}}^2 \end{aligned} \right\}$$

Estimated errors for these and other terms in (1.1) and (1.2) are shown in subsequent figures.

### 3. Mean and eddy kinetic energy

Distribution of the streamfunction (100/1000 db) of mean flow is shown in Fig. 1. Contour intervals are larger than twice the error estimates. This pattern essentially corresponds to the long-term mean map of temperature at 300 m, produced by Bernstein and White (1981). Major characteristics of this mean flow are described in that article. Among them are quasi-stationary waves in the mean flow, and the apparent topographic influence of the Shatsky Rise. This latter topographic feature runs approximately in a northeast-southwest direction, centered at  $\sim 160^\circ\text{E}$  longitude. Mean flow upstream (west) of

the Shatsky Rise has a mean southward component but east of there the flow is zonal.

The mean kinetic energy field is shown in Fig. 2, where it alternately increases and decreases along the mean axis of the current, superimposed upon a decreasing trend to the east. Maximum mean kinetic energy of  $500 \text{ cm}^2 \text{ s}^{-2}$  occurs near  $36^\circ\text{N}, 146^\circ\text{E}$ ; east of there, it decreases along the streamlines shown in Fig. 1, reaching a minimum value of  $50 \text{ cm}^2 \text{ s}^{-2}$  near  $155^\circ\text{E}$ , one-tenth of the maximum value to the west. Proceeding eastward from that point, mean kinetic energy intensifies again, reaching a secondary maximum value at  $35^\circ\text{N}, 159^\circ\text{E}$ . This location is the site of a deep passage through the Shatsky Rise, and has been shown by Bernstein and White (1981) to be a favorable path for the Kuroshio Extension.

East of the Shatsky Rise, mean kinetic energy decreases monotonically as flow proceeds in the gen-

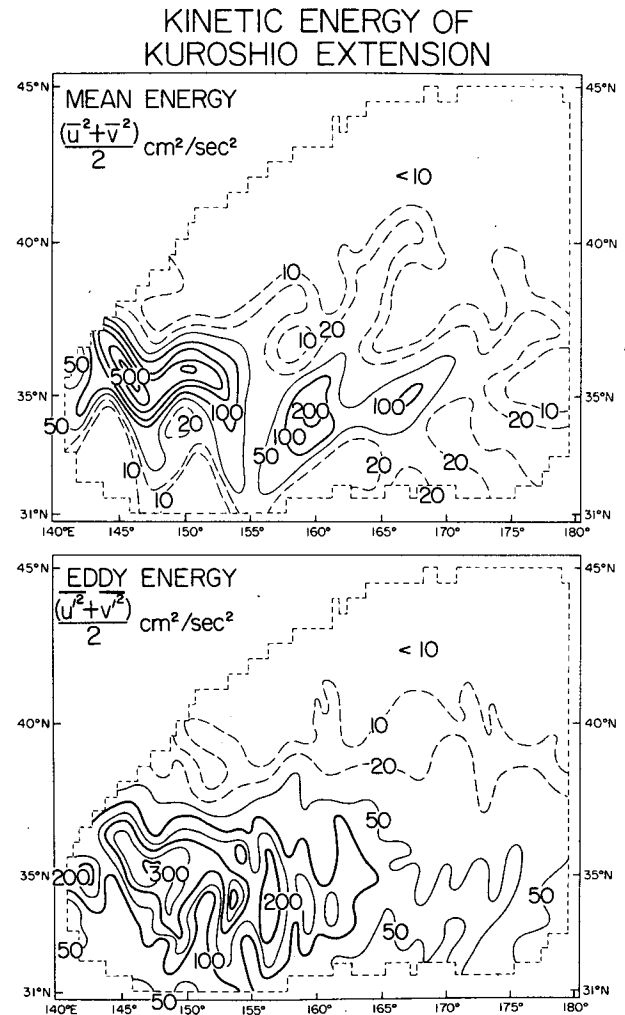


FIG. 2. Horizontal distribution of horizontal mean kinetic energy and horizontal eddy kinetic energy. Solid contour interval of the mean field exceeds twice the standard error, but for the eddy field it exceeds only the standard error.

eral eastward direction. By following spatial maxima in the kinetic energy, the mean flow can be seen to bifurcate east of the Shatsky Rise at  $163^\circ\text{E}$ , with a secondary branch extending in the northeastern direction. Another bifurcation takes place at the Emperor Seamount Chain at  $172^\circ\text{E}$ , with two filaments of almost equal strength extending eastward at  $37$  and  $32^\circ\text{N}$ .

The eddy kinetic energy field is shown in Fig. 2 as well. It shows most eddy activity occurring west of the Shatsky Rise, with a sharp decrease to the east. Within both subregions (i.e., west and east of the Shatsky Rise) eddy kinetic energy is generally larger where mean kinetic energy is larger, with one major exception near  $156^\circ\text{E}$ .

Kinetic energy of the mean flow and of "eddies" calculated by Wyrki *et al.* (1976) shows comparable values in the mean (e.g.,  $\approx 200 \text{ cm}^2 \text{ s}^{-2}$ ), but larger values in eddy kinetic energy (e.g.,  $\approx 600 \text{ cm}^2 \text{ s}^{-2}$ ). This discrepancy in the eddy kinetic energy may be due to differences in the character of data used. The ship-drift data measures direct wind-driven currents, in addition to the geostrophic ones measured here, and is contaminated by wind-ship interaction. Moreover, ship-drift data for 72 years were used; this means that eddy energy contains larger scale, year-to-year, variability in geostrophic flow. Large-scale interannual changes have been shown by White (1977) to be more energetic than mesoscale variability.

Computed meridional profiles of zonally-averaged values are shown in Fig. 3. With large differences in eddy kinetic energy between the regions west and

east of the Shatsky Rise, zonal averages are constructed for each subregion separately. West of the Shatsky Rise, mean flow extends along an axis that is oriented slightly south of east; therefore, zonal mean there is taken along the line shown in Fig. 1. All subsequent computations in this region are rotated from the east-west direction to the coordinate system shown in Fig. 1. Henceforth, zonal mean ( $\langle \rangle$ ) is referenced along the line in Fig. 1 west of the Shatsky Rise, but along latitude lines east of the Shatsky Rise.

The meridional profile of zonally-averaged eddy kinetic energy ( $\frac{1}{2}\langle \overline{u'^2 + v'^2} \rangle$ ) is shown in Fig. 3 together with that of zonally-averaged eastward mean flow ( $\langle \overline{u} \rangle$ ) for each subregion. Two peaks of eddy kinetic energy and of mean eastward flow, respectively, occur at nearly the same latitude in both subregions, indicative of strongest eddy activity occurring in the strongest part of the mean flow. The difference between western and eastern subregions is in the intensity of these peaks.

#### 4. Horizontal eddy flux of momentum

Horizontal flux of momentum is partitioned among horizontal tensor components of  $u'_i u'_j$  (i.e.,  $\overline{u'^2}$ ,  $\overline{v'^2}$ , and  $\overline{u'v'}$  in the more usual notation). Of these three terms, the gradient of the cross-stream term (i.e.,  $\overline{u'v'}$ ) is usually considered to have the most important effect upon the mean momentum balance. But, in this situation, mean flow diverges to the east and contains a number of quasi-stationary meanders, in which case downstream terms (i.e.,  $\overline{u'^2}$ ,  $\overline{v'^2}$ ) have gra-

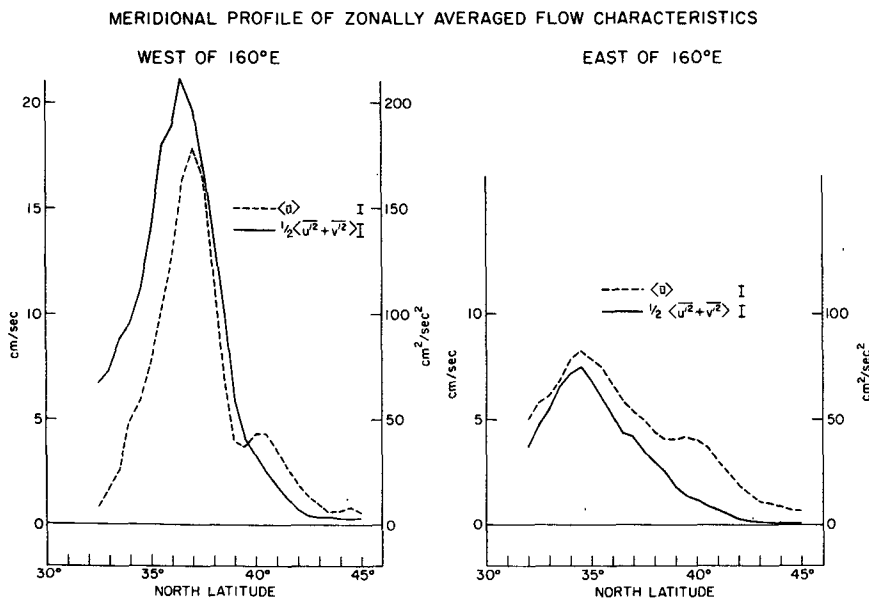


FIG. 3. Meridional profile of mean zonal flow, together with eddy kinetic energy, zonally averaged for both subregions east and west of the Shatsky Rise. Standard error estimates are given as shown.

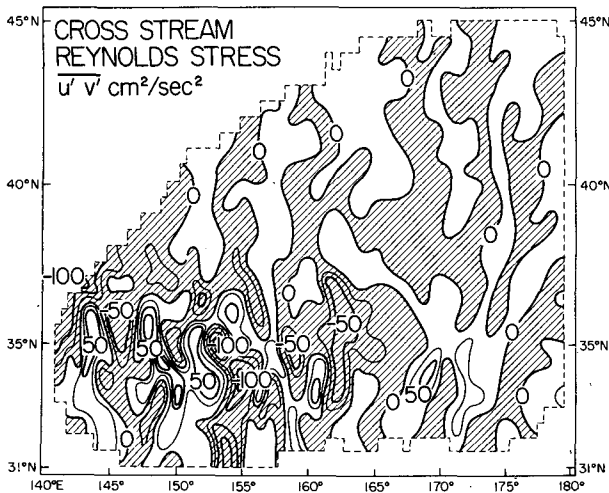


FIG. 4. Horizontal distribution of the cross-stream, horizontal momentum flux ( $\overline{u'v'}$ ). The solid contour intervals exceed twice the standard error.

dients that play an important role in the transport of momentum according to (1.1).

Distribution of  $\overline{u'v'}$  (Fig. 4) over the entire region of interest shows great variety from place to place, with both negative and positive values distributed as indicated. The pattern of this variety seems to correspond to quasi-stationary meanders in mean flow; i.e., a tendency exists for  $\overline{u'v'}$  to be positive on the downstream side of wave crests and to be negative

on the upstream side. In addition, these stresses tend to be mostly negative over the Shatsky Rise near 160°E.

Meridional profiles of zonally averaged values of  $\overline{u'v'}$  and  $\overline{v'^2}$  are shown in Fig. 5. The profile of  $\langle \overline{u'v'} \rangle$  is a negative on the north side of the axis of mean flow and positive on the south side in both the western and eastern subregions. This means that mean zonal momentum is transported northward on the south side of the axis of mean flow and southward on the north side. As a result, the cross-stream term of the horizontal Reynolds stress tensor has a tendency to intensify the mean flow. This result is similar to that of Webster (1961, 1965) in the Gulf Stream south of Cape Hatteras. Schmitz (1977) showed a similar result from his deep moored current meters located in the Gulf Stream east of Cape Hatteras. In Holland's (1978) eddy-resolving model, a similar tendency existed in the eastward extension of western boundary currents. On the other hand, Szabo and Weatherly (1979) conducted a study similar to that of Webster's in the Kuroshio south of Japan, finding the opposite result. However, the Kuroshio in this part of the western boundary region is known (Taft, 1972) to be relatively free of transient mesoscale variability.

A strong peak in  $\langle \overline{v'^2} \rangle$  appears in Fig. 5 near the axis of mean flow in both subregions. Sharp gradients on either side of the flow axis indicate the presence of forces that tend to increase mean north-south momentum on the north side of the axis and tend to

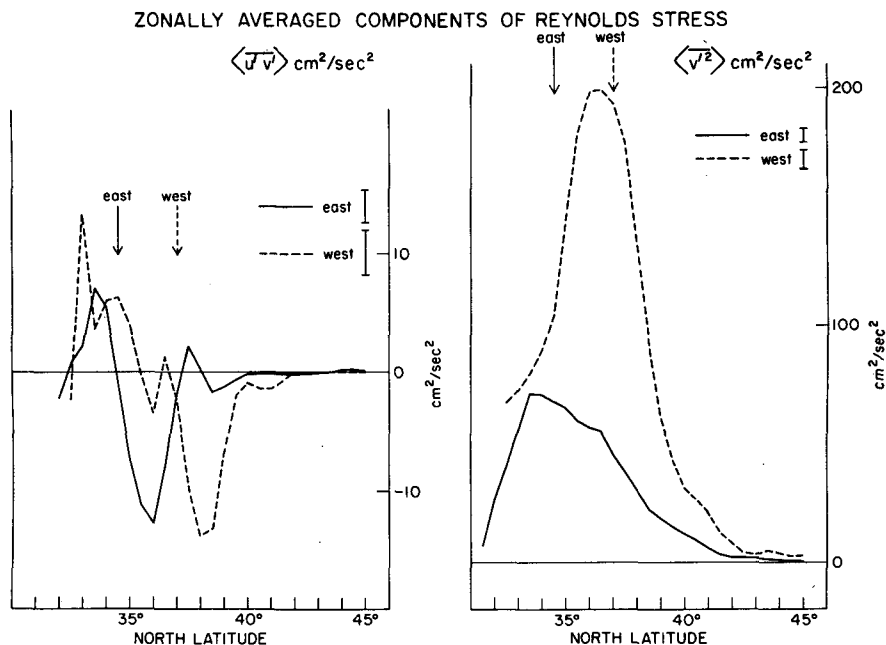


FIG. 5. Meridional profiles of  $\langle \overline{u'v'} \rangle$  and  $\langle \overline{v'^2} \rangle$  displayed individually for both subregions east and west of the Shatsky Rise. The arrows indicate the axis of the mean flow. Standard errors are given as shown.

decrease it on the south side. This results in a tendency for spreading of the mean flow.

### 5. Horizontal momentum flux by quasi-stationary meanders

When the mean momentum balance is zonally averaged, zonally averaged momentum fluxes due to *transient* mesoscale variability represent only part of the horizontal momentum flux. Another part is associated with the spatial correlation of  $\bar{u}$  and  $\bar{v}$ . These were discovered in the study of the zonally averaged atmospheric angular momentum balance by Starr and White (1952). These fluxes arise from consideration of zonally averaged momentum transport  $\langle \bar{u}\bar{v} \rangle$ :

$$\langle \bar{u}\bar{v} \rangle = \langle \bar{u} \rangle \langle \bar{v} \rangle + \langle \bar{u}'\bar{v}' \rangle + \langle \bar{u}'\bar{v}' \rangle. \quad (5.1)$$

The first term on the right-hand side of this expression represents momentum transport by the zonally-averaged mean motion and the third term zonally-averaged momentum transport by transient mesoscale variability, already discussed. The second term is a zonally-averaged momentum flux associated with the asymmetry of trough and ridges in the quasi-stationary meanders of the mean flow (Machta, 1949).

Values of  $\langle \bar{u}'\bar{v}' \rangle$  in both the western and eastern subregions are plotted in Fig. 6. In the western subregion negative momentum flux exists on the south side of the axis of mean flow, with positive flux on the north side. However, the latter is so much smaller than the former that net momentum flux over the mean flow width is negative (i.e., southward). In the eastern subregion, no clear tendency of momentum flux is evident. Quasi-stationary meanders found in mean flow in the western subregion (see Fig. 1) exhibit a significant departure from a sinusoid, with a general northwest-southeast tilt of trough lines, particularly on the south side of the axis of mean flow. Tilt in this direction, according to Machta (1949), is associated with southward flux of mean zonal momentum, the same as with the quantitative results.

### 6. Mean kinetic energy tendency

Eddy processes play two roles in the mean kinetic energy balance of a current (i.e., kinetic energy exchange and kinetic energy redistribution) as indicated in (1.3). The former acts as a source or sink of mean kinetic energy, and the latter does work to redistribute it. These two effects combined give the total mean kinetic energy tendency due to eddy processes [see (1.2)]. In addition to eddy processes that tend to alter the mean kinetic energy, there also exist (see 1.2) a tendency to do the same through advection of the mean kinetic energy by the mean flow

### MERIDIONAL MOMENTUM TRANSPORT BY QUASI-STATIONARY MEANDERS

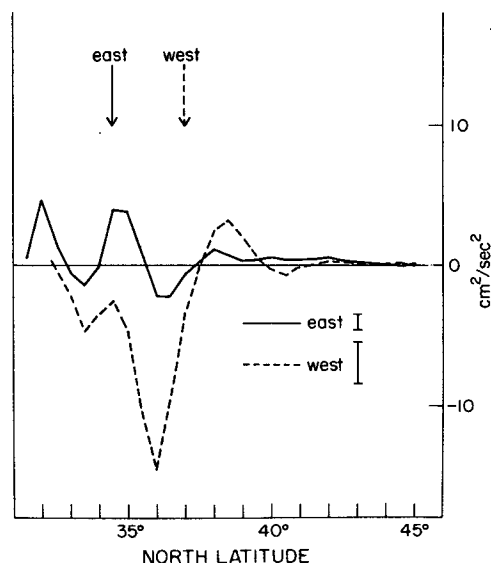


FIG. 6. Meridional profiles of  $\langle \bar{u}'\bar{v}' \rangle$  for both subregions east and west of the Shatsky Rise. The arrows indicate the axis of the mean flow. Standard errors are given as shown.

itself; this is estimated below. The mean kinetic energy balance cannot be closed because of lack of observation of pressure, vertical velocity and the coefficients of turbulent diffusion.

#### a. Horizontal mean energy advection

Zonally-averaged mean kinetic energy advection by horizontal mean flow is represented by  $\langle \bar{u}_j \partial / \partial x_j (\bar{u}_i \cdot \bar{u}_i) / 2 \rangle$  in (1.2), neglecting terms involving  $\bar{w}$ , and can be expressed in the usual notation:

$$\left\langle \bar{u}_j \frac{\partial}{\partial x_j} \left( \frac{\bar{u}_i \cdot \bar{u}_i}{2} \right) \right\rangle = \left\langle \bar{u} \frac{\partial}{\partial x} \left( \frac{\bar{u}^2 + \bar{v}^2}{2} \right) \right\rangle + \left\langle \bar{v} \frac{\partial}{\partial y} \left( \frac{\bar{u}^2 + \bar{v}^2}{2} \right) \right\rangle. \quad (6.1)$$

Meridional profiles of this quantity are given in Fig. 7 for both subregions.

In the eastern subregion horizontal advection is negative all across the mean flow, tending to increase the mean kinetic energy at a point. However, following a streamline, it is indicative of a reduction in mean kinetic energy in the downstream direction, coincident with that observed in Figs. 1 and 2.

In the western subregion, horizontal advection is positive near the axis of mean flow and negative on either side, tending to decrease the mean kinetic energy near the axis of the current, and increase it on the flanks. However, following a streamline, it is in-

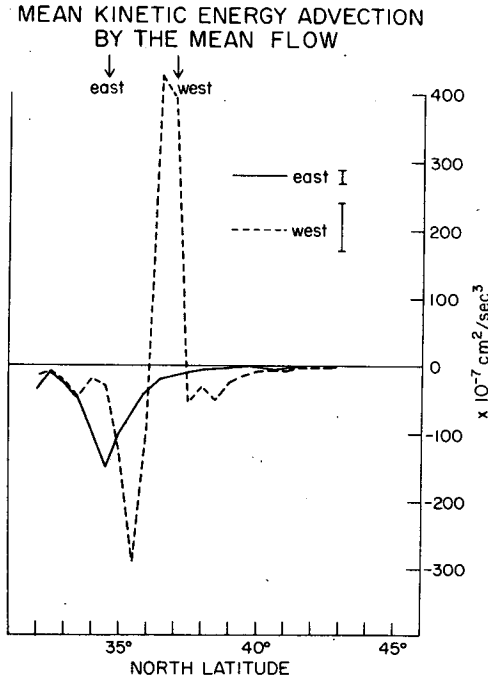


FIG. 7. Meridional profiles of  $\langle \bar{u}_j \partial / \partial x_j (\bar{u}_i \cdot \bar{u}_i) / 2 \rangle$  for both subregions east and west of the Shatsky Rise. The arrows indicate the axis of the mean flow. Standard errors are given as shown.

dicative of an increase in kinetic energy in the downstream direction near the axis of the current.

### b. Horizontal kinetic energy exchange

Zonally-averaged, horizontal kinetic energy exchange between mesoscale variability and the mean flow is represented by  $\langle \bar{u}'_i \bar{u}'_j \partial \bar{u}_i / \partial x_j \rangle$  in (1.3), neglecting the terms involving  $w'$  and  $\bar{w}$ , and can be expressed in the usual notation:

$$\langle \bar{u}'_i \bar{u}'_j \frac{\partial \bar{u}_i}{\partial x_j} \rangle = \left\langle \overline{u'v'} \frac{\partial \bar{u}}{\partial y} \right\rangle + \left\langle \overline{u'v'} \frac{\partial \bar{v}}{\partial x} \right\rangle + \left\langle \overline{u'^2} \frac{\partial \bar{u}}{\partial x} \right\rangle + \left\langle \overline{v'^2} \frac{\partial \bar{v}}{\partial y} \right\rangle. \quad (6.2)$$

Meridional profiles of zonally-averaged values of each term of horizontal kinetic energy exchange are given in Fig. 8 for the two subregions. The net horizontal kinetic energy exchange [i.e., the sum of the four terms in (6.2)] is profiled in Fig. 9 for both subregions.

The net horizontal kinetic energy exchange is positive on the north side of the axis of mean flow and negative on the south side. This means that north of the axis of mean flow, mean kinetic energy tends to increase at the expense of eddy kinetic energy, but on the south the opposite takes place.

Individual terms in (6.2) have the following meridional profiles. The term  $\langle \overline{u'v'} \partial \bar{u} / \partial y \rangle$  generally is

positive over the entire latitude range in both subregions. This is expected from the result in the previous section, where the signs of  $\bar{u}'v'$  and  $\partial \bar{u} / \partial y$  are the same. These positive values tend to increase the mean kinetic energy everywhere. Both subregions have a similar tendency, but with a reduction in magnitude from west to east.

The term  $\langle \overline{u'v'} \partial \bar{v} / \partial x \rangle$  is negative on the south side of the axis of mean flow and positive on the north side (nearly) for both subregions. Magnitudes are comparable with the previous term  $\langle \overline{u'v'} \partial \bar{u} / \partial y \rangle$ , which in the past (e.g., Webster, 1961) was considered largest of the horizontal kinetic energy exchange terms.

A distinct tendency exists for terms  $\langle \overline{u'^2} \partial \bar{u} / \partial x \rangle$  and  $\langle \overline{v'^2} \partial \bar{v} / \partial y \rangle$  to cancel each other at each location in the meridional profile. This is particularly clear in the eastern region and is expected under ideal conditions; i.e., in isotropic turbulence  $\bar{u}'^2$  is equal to  $\bar{v}'^2$  and with zero horizontal divergence, then  $\overline{u'^2} \partial \bar{u} / \partial x$  is equal but opposite to  $\overline{v'^2} \partial \bar{v} / \partial y$ . Even in the present anisotropic situation, when these two terms are summed, it equals zero to within the error limits of estimation.

Terms  $\langle \overline{u'v'} \partial \bar{u} / \partial y \rangle$  and  $\langle \overline{u'^2} \partial \bar{u} / \partial x \rangle$  in (6.2) are associated with exchange of zonal kinetic energy between mean flow and mesoscale variability. Fig. 8 shows that the sum over all latitudes of these two terms is negative, indicating that zonal mean kinetic energy tends to decrease. Terms  $\langle \overline{u'v'} \partial \bar{v} / \partial x \rangle$  and  $\langle \overline{v'^2} \partial \bar{v} / \partial y \rangle$  in (6.2) are associated with exchange of meridional kinetic energy between mean flow and mesoscale variability. Fig. 8 shows that the sum over all latitudes of  $\overline{u'v'} \partial \bar{v} / \partial x$  and  $\overline{v'^2} \partial \bar{v} / \partial y$  is positive, indicating that meridional mean kinetic energy is tending to increase. While this is consistent with the tendency in the zonal and meridional mean kinetic energy in the downstream direction (i.e., inferred from Fig. 1), it does not represent the total effect of eddy processes upon the mean flow.

### c. Horizontal mean kinetic energy redistribution

Zonally-averaged, horizontal, mean kinetic energy redistribution is represented by  $\langle \partial / \partial x_j (\bar{u}'_i \bar{u}'_j \cdot \bar{u}_i) \rangle$  in (1.3), neglecting the terms involving  $w'$  and  $\bar{w}$ , and can be expressed in the usual notation:

$$\begin{aligned} & - \left\langle \frac{\partial}{\partial x_j} (\bar{u}'_i \bar{u}'_j \cdot \bar{u}_i) \right\rangle \\ & = - \left\langle \frac{\partial}{\partial y} (\overline{u'v'} \cdot \bar{u}) \right\rangle - \left\langle \frac{\partial}{\partial x} (\overline{u'^2} \cdot \bar{u}) \right\rangle \\ & \quad - \left\langle \frac{\partial}{\partial x} (\overline{u'v'} \cdot \bar{v}) \right\rangle - \left\langle \frac{\partial}{\partial y} (\overline{v'^2} \cdot \bar{v}) \right\rangle. \quad (6.3) \end{aligned}$$

Meridional profiles of the zonal mean value of each term in the above expression are given in Fig. 10 for

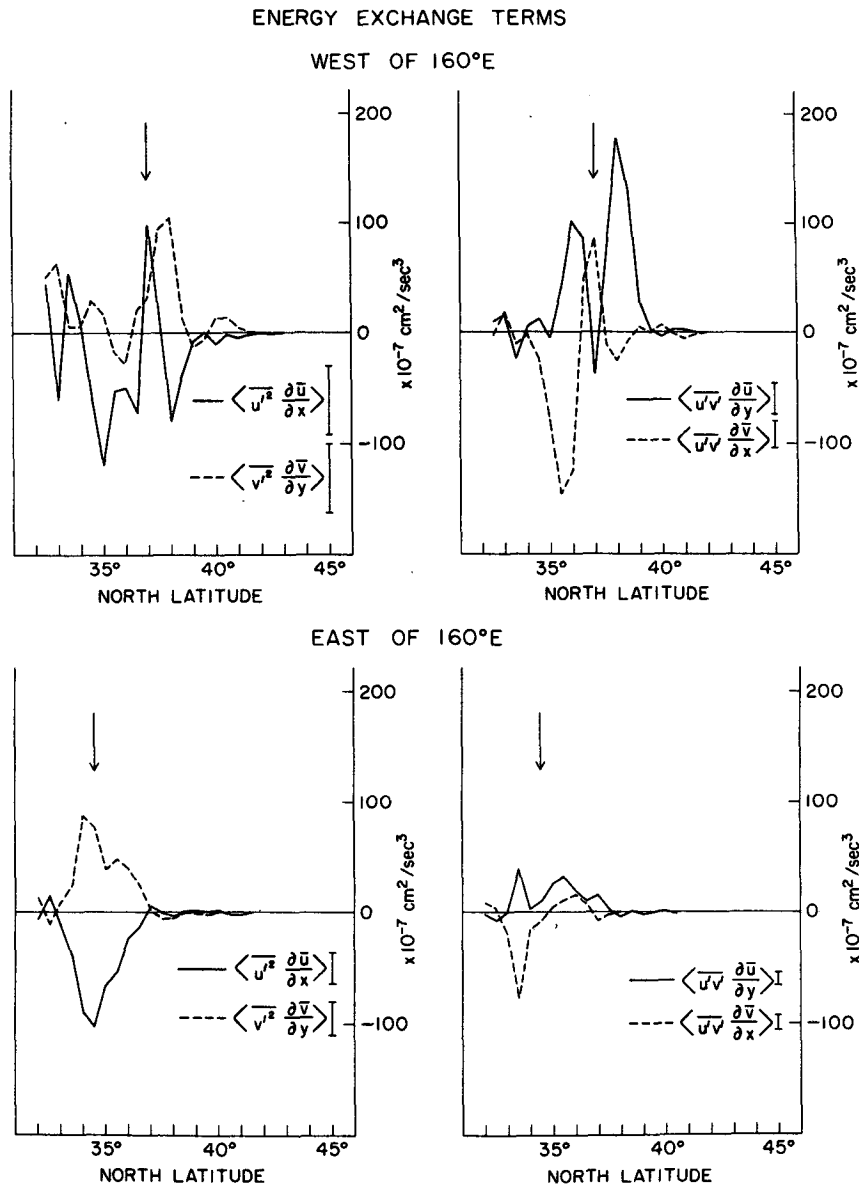


FIG. 8. Meridional profiles of the horizontal kinetic energy exchange terms, zonally averaged for both subregions east and west of the Shatsky Rise. The arrows indicate the axis of the mean flow. Standard errors are given as shown.

the eastern subregion only. The western subregion is excluded from display, because of their noise-like appearance. The net amount of kinetic energy redistribution for both subregions is profiled in Fig. 11.

In the eastern subregion, net horizontal mean kinetic energy redistribution shown in Fig. 11 is positive over all latitudes, meaning that mean kinetic energy converges due to the stresses of the mesoscale variability. Upon inspection of each of the component terms in Fig. 10,  $\langle -\partial/\partial x(\bar{u}^2 \cdot \bar{u}) \rangle$  is dominant, associated with the downstream momentum transport  $\bar{u}^2$ . As such, the downstream stress is more important

than the cross-stream stress in the net redistribution of the horizontal mean kinetic energy.

In the western subregion the net horizontal mean kinetic energy redistribution profiled in Fig. 10 displays nearly random fluctuations.

### 7. Conclusion

East of Japan, the Kuroshio Extension in the subregion west of the Shatsky Rise intensifies near the axis of mean flow, but eastward of the Rise exhibits a gradual weakening and spreading of the



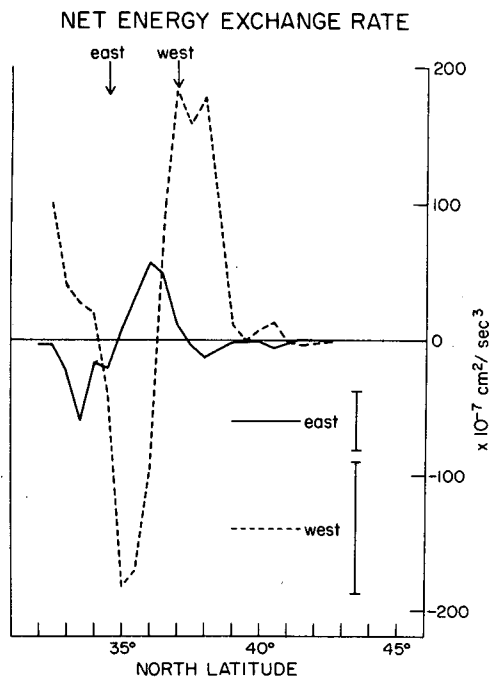


FIG. 9. Meridional profiles of net horizontal kinetic energy exchange, zonally averaged for both subregions east and west of the Shatsky Rise. The arrows indicate the axis of the mean flow. Standard errors are given as shown.

streamlines, associated with a considerable decrease in zonal mean kinetic energy and a slight increase in meridional mean kinetic energy. Eddy kinetic energy is largest near the axis of the Kuroshio Extension, showing a maximum in the west, and decreasing rapidly east of the Shatsky Rise near  $160^{\circ}\text{E}$ .

Zonally averaged, cross-stream, horizontal eddy momentum flux  $\langle \bar{u}'v' \rangle$  is negative in both subregions on the north side of the axis of mean flow and positive on the south side, and tends to converge eastward mean momentum, which is greatest at the axis. This result is in agreement with that of Webster (1961) for the Gulf Stream south of Cape Hatteras, but not with that of Szabo and Weatherly (1979) for the Kuroshio south of Japan.

In the zonally-averaged mean momentum balance for the Kuroshio Extension a horizontal momentum flux component arises from asymmetry of the quasi-stationary meanders in the Kuroshio Extension. In the western subregion these fluxes are negative on the south side of the axis and slightly positive on the north side. This profile is opposite in sign to that due to transient eddy processes in the subregion, and therefore reduces the tendency of the latter to increase the zonally averaged eastward mean flow there. In the eastern subregion, quasi-stationary meanders are much reduced in amplitude and have no clear influence on the zonally-averaged mean eastward flow.

A comparison of the strengths of these horizontal eddy processes in bringing about convergence or divergence of momentum in zonally-averaged eastward mean flow in the region west of the Shatsky Rise is made in Table 1, for the regions both north and south of, and on, the axis of the Kuroshio Extension, according to (1.1). These terms almost cancel one another on the axis and on the south side of the axis; however, on the north side transient momentum fluxes act to converge zonally-averaged eastward mean flow, dominating the divergent tendency of the quasi-stationary fluxes. This might account for the asymmetry in the meridional profile of the zonally-averaged mean flow of the Kuroshio Extension (see Fig. 3), which intensifies on the north side of the axis.

In the mean kinetic energy balance expressed in (1.2) are three terms that can be estimated from the present data base. These are the horizontal mean advection of the mean kinetic energy, the redistribution of horizontal mean kinetic energy, and the exchange of horizontal kinetic energy between the mean flow and the mesoscale variability. Vertical eddy and mean processes could not be estimated. Mean advection of the mean kinetic energy tends to increase horizontal mean kinetic energy in the subregion east of the Shatsky Rise. In the western subregion, mean advection tends to decrease horizontal mean kinetic energy near the axis but to increase it on the flanks. The horizontal kinetic energy exchange between the mean flow and mesoscale variability tends to increase the mean kinetic energy on the north side of the axis of mean flow and to decrease it on the south side in both subregions. Of the four terms that contribute to horizontal kinetic energy exchange in (6.2), all have comparable magnitudes. Redistribution of horizontal mean kinetic energy tends to increase horizontal mean kinetic energy in the eastern subregion, particularly on the south side of the axis. In the western subregion, big fluctuations occur over the entire width of the Kuroshio Extension, with no consistent relation to the mean flow.

A comparison between these three tendencies in the mean kinetic energy balance is given in Table 2, in which overall means (i.e., averaged in  $x$ ,  $y$ , and  $t$ ) are given for both subregions. In the eastern subregion, horizontal advection of mean kinetic energy by the mean flow and the redistribution of horizontal kinetic energy by eddy processes have positive tendencies upon the mean kinetic energy balance, dominating the kinetic energy exchange tendency. In the western subregion, the redistribution and exchange tendencies dominate the advection tendency, but are of opposite signs, so that the overall effect of horizontal eddy processes is small.

Residual kinetic energy tendencies shown in the last column of Table 2, may represent those of other terms of the mean kinetic energy balance not included in this investigation. These include the time

INDIVIDUAL TERMS OF THE MEAN KINETIC ENERGY REDISTRIBUTION BY REYNOLDS STRESSES

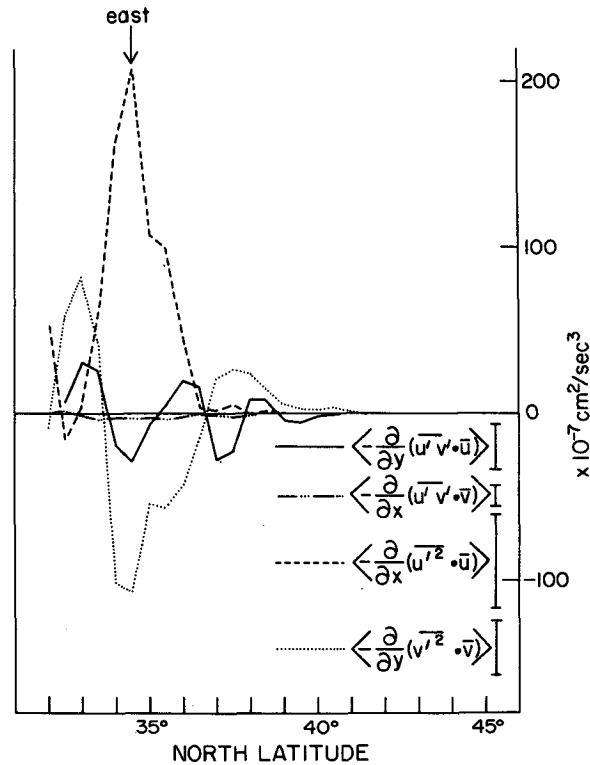


FIG. 10. Meridional profiles of the horizontal mean kinetic energy redistribution terms, zonally averaged for the subregion east of the Shatsky Rise. The arrows indicate the axis of the mean flow. Standard errors are given as shown.

change of mean flow, effects of vertical eddy processes, interaction with subgrid variability, and the influence of pressure forces. Of particular importance is that, while the western subregion has much stronger mean and eddy kinetic energy than the eastern subregion, the latter subregion displays much larger values of mean kinetic energy tendencies. This means that the principal kinetic energy interaction between the mean flow and mesoscale variability takes place east of the Shatsky Rise (i.e., 160°E).

In the Kuroshio Extension,  $\partial\bar{u}/\partial x$ ,  $\partial\bar{v}/\partial y$ ,  $\partial\bar{v}/\partial x$  are not negligible compared with  $\partial\bar{u}/\partial y$ ; therefore, estimation of eddy viscosity, in order to parameterize eddy processes in terms of mean flow characteristics,

leads to a contradictory result (Heinze, 1959). Horizontal eddy viscosity cannot be parameterized in either analytical or numerical models of the Kuroshio Extension. Rather, mesoscale variability itself must be modeled directly, yielding a statistical relationship with the mean flow that agrees with that reported here.

Upon examination of sources of error in these calculations, increasing the sampling density by a factor of four (from 100 to 50 km sampling intervals) will improve accuracy of the statistics by only 20%. On the other hand, doubling the length of time of the sampling program at the existing sampling density improves accuracy of the statistics by only 30%. As such, reduction of errors in this kind of analysis be-

TABLE 1. Comparison of transient and stationary horizontal eddy momentum fluxes in the western region.

|                    | $-\frac{\partial}{\partial y} \langle \overline{u'v'} \rangle$<br>( $\times 10^{-7} \text{ cm s}^{-2}$ ) | $-\frac{\partial}{\partial y} \langle \overline{u'v'} \rangle$<br>( $\times 10^{-7} \text{ cm s}^{-2}$ ) |
|--------------------|--|--|
| North side of axis | $-5.0 \pm 1.3$   | $1.2 \pm 0.8$  |
| At the axis        | $5.2 \pm 3.7$  | $-6.3 \pm 2.7$   |
| South side of axis | $-4.3 \pm 3.7$   | $5.2 \pm 2.5$  |

TABLE 2. Comparison of mean kinetic energy tendencies.

|               | Advection<br>( $\times 10^{-7} \text{ cm}^2 \text{ s}^{-3}$ ) | Redistribution<br>( $\times 10^{-7} \text{ cm}^2 \text{ s}^{-3}$ ) | Exchange<br>( $\times 10^{-7} \text{ cm}^2 \text{ s}^{-3}$ ) | Residual<br>( $\times 10^{-7} \text{ cm}^2 \text{ s}^{-3}$ ) |
|---------------|---|--|--|--|
| East of 160°E | $24 \pm 3$  | $43 \pm 11$  | $1 \pm 6$  | $-68 \pm 13$   |
| West of 160°E | $1 \pm 10$  | $-10 \pm 16$   | $15 \pm 27$  | $-6 \pm 33$  |

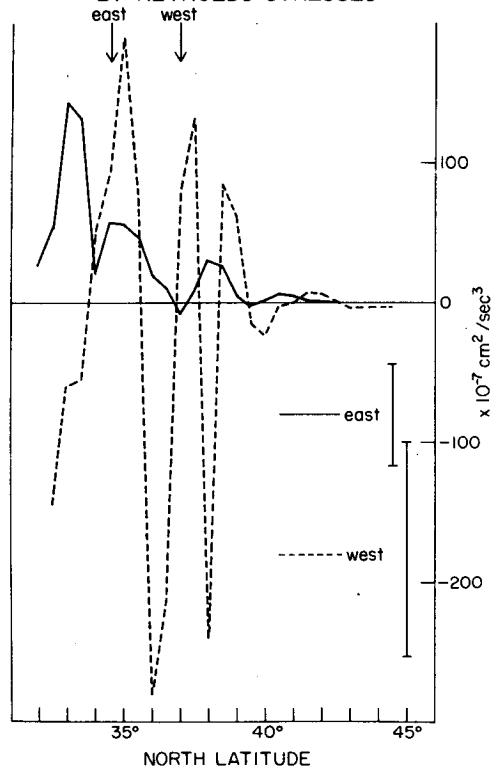
NET MEAN KINETIC ENERGY REDISTRIBUTION  
BY REYNOLDS STRESSES

FIG. 11. Meridional profiles of net horizontal mean kinetic energy redistribution, zonally averaged for both subregions east and west of the Shatsky Rise. The arrows indicate the axis of the mean flow. Standard errors are given as shown.

yond 20–30% is either not feasible at this time or far off in the future. Therefore, it is not possible, using this XBT data base, to determine the horizontal distribution of the horizontal eddy processes affecting the mean kinetic energy balance. The limiting factor in this is the large errors incurred when inferring dynamic height and geostrophic velocities from temperature data alone. Much of this error can be reduced by determining current velocities directly, using horizontal current meter arrays. Because of the suggestion in Fig. 4 that the horizontal eddy processes affecting the mean kinetic energy balance are different for different longitudinal locations in the Kuroshio Extension, these arrays should contain longitudinal as well as latitudinal coverage.

*Acknowledgments.* Much gratitude is extended to Ted Walker who, as programmer, made the calculation of geostrophic velocities used in this study.

The Science and Technology Agency of Japan provided funds, making it possible for the principal author to conduct this research at Scripps Institution of Oceanography.

The research at Scripps Institution was sponsored by the Office of Naval Research under ONR contract N00014-75-C-0152 and by the University of California, San Diego, Scripps Institution of Oceanography through NORPAX.

## REFERENCES

- Bernstein, R. L., and W. B. White, 1981: Stationary and traveling mesoscale perturbations in the Kuroshio Extension current. *J. Phys. Oceanogr.*, **11**, 692–704.
- Hager, J. G., 1977: Kinetic energy exchange in the Gulf Stream. *J. Geophys. Res.*, **82**, 1718–1724.
- Harrison, D. E., and A. R. Robinson, 1978: Energy analysis of open ocean regions of turbulent flows—mean eddy energetics of a numerical ocean circulation experiment. *Dyn. Atmos. Oceans*, **2**, 185–211.
- Heinze, J. D., 1959: *Turbulence*. McGraw-Hill, 586 pp.
- Holland, W. R., 1978: The role of mesoscale eddies in the general circulation of the ocean—numerical experiments using a wind-driven quasi-geostrophic model. *J. Phys. Oceanogr.*, **8**, 363–392.
- Lumley, J. L., and H. A. Panofsky, 1964: *The Structure of Atmospheric Turbulence*. Interscience, 231 pp.
- Machta, L., 1949: Dynamic characteristics of a tilted-trough model. *J. Meteor.*, **6**, 261–265.
- Schmitz, W. J., 1977: On the deep general circulation in the western North Atlantic. *J. Mar. Res.*, **35**, 21–28.
- Starr, V., and R. White, 1952: A hemispherical study of the atmospheric angular momentum balance. *Quart. J. Roy. Meteor. Soc.*, **77**, 66–76.
- Szabo, D., and G. L. Weatherly, 1979: Energetics of the Kuroshio south of Japan. *J. Mar. Res.*, **37**, 531–556.
- Taft, B. A., 1972: *Characteristics of the Flow of the Kuroshio South of Japan. Kuroshio: Its Physical Aspect*. University of Tokyo Press, 517 pp.
- Webster, F., 1961: The effect of meanders on the kinetic energy balance of the Gulf Stream. *Tellus*, **13**, 392–401.
- , 1965: Measurements of eddy fluxes of momentum in the surface layer of the Gulf Stream. *Tellus*, **17**, 239–245.
- White, W. B., 1977: Secular variability in the baroclinic structure of the interior North Pacific from 1950–1970. *J. Mar. Res.*, **35**, 587–607.
- , and R. L. Bernstein, 1979: Design of an oceanographic network in the mid-latitude North Pacific. *J. Phys. Oceanogr.*, **9**, 592–606.
- Wyrtki, K. L., L. Maggaard and J. Hager, 1976: Eddy energy in the oceans. *J. Geophys. Res.*, **81**, 2641–2646.